Brain Imaging and Behavior (2017) 11:176–184
DOI 10.1007/s11682-016-9518-5

ORIGINAL RESEARCH

Aberrant regional homogeneity of resting-state executive control, default mode, and salience networks in adult patients with moyamoya disease

Yu Lei[1] · Jiabin Su[1] · Hanqiang Jiang[1] · Qihao Guo[2] · Wei Ni[1] · Heng Yang[1] · Yuxiang Gu[1] · Ying Mao[1]

Published online: 3 February 2016

Abstract Aberrant local connectivity within cerebral intrinsic connectivity networks (ICNs) at rest has not been reported in adult moyamoya disease (MMD). Our aim was to examine the regional homogeneity (ReHo) of executive control (ECN), default mode (DMN), and salience networks (SN) in patients with executive dysfunction to explore the underlying mechanism. Twenty-six adult patients with MMD and 24 normal control (NC) subjects were recruited. Executive function was evaluated by Trail Making Test Part B (TMT-B) and executive subtests of Memory and Executive Screening (MES-EX). Compared with NC, the case group exhibited ReHo decrease mainly in the frontal and parietal gyrus, and increase only in the left middle temporal gyrus. Subsequent ICNs analysis indicated that compared with NC, patients with MMD exhibited significantly decreased ReHo in the dorsolateral prefrontal cortex (DLPFC) and inferior parietal gyrus (IPG) of left ECN; the IPG, superior frontal gyrus, and DLPFC of the right ECN; the right precuneus, left medial superior frontal gyrus, and right medial orbitofrontal gyrus of the DMN; as well as the left middle frontal gyrus and right supplemental motor area of SN. When referring to the Suzuki's 6-stage classification, a trend of ReHo decrease with disease severity was observed in all of the ICNs examined, but only bilateral ECNs reached statistical significance. Finally, only bilateral ECNs exhibited a significant correlation of averaged ReHo values with executive performance. Our results provide new insight into the pathophysiology of adult MMD.

Keywords Executive function · Functional magnetic resonance imaging · Moyamoya disease · Regional homogeneity

Introduction

A large number of neuropsychological studies have addressed the issue of vascular cognitive impairment in adult patients with moyamoya disease (MMD) (Festa et al. 2010; Karzmark et al. 2008; Weinberg et al. 2011). Vascular cognitive impairment is a syndrome characterized by subclinical cerebral vascular defects or clinical stroke and neurocognitive impairment, affecting at least one cognitive domain of executive function/attention, memory, language, and visuospatial functions (Gorelick et al. 2011). Executive function is considered to be predominantly impaired in adult MMD, but the underlying neural mechanism is still unknown.

Neuroimaging studies have demonstrated that the intrinsic connectivity networks (ICNs) play important roles in cognitive processing, such as bilateral executive control networks (ECNs), default mode network (DMN), and salience network (SN) (Bressler and Menon 2010; Cocchi et al. 2014; Liang et al. 2015). Although recent articles have already noted contributions of these ICNs to normal executive control performance, their aberrant functional activity in executive defects is still unclear, especially in adult MMD (Liang et al. 2015; Xin and Lei 2015).

Yu Lei and Jiabin Su contributed equally to this work.

✉ Yuxiang Gu
709586957@qq.com

[1] Department of Neurosurgery, Huashan Hospital of Fudan University, Wulumuqi Zhong Road 12, Shanghai 200040, China

[2] Department of Neurology, Huashan Hospital of Fudan University, Shanghai 200040, China

The neuronal baseline activity of the brain can be presented by resting-state function MRI (fMRI). In a previous study, we preliminarily demonstrated that adult MMD exhibits a specific functional pattern of amplitude of low-frequency fluctuations and this pattern changes following cognitive impairment (Lei et al. 2014). However, little is known about the aberrant local connectivity within resting-state ICNs with respect to adult MMD with executive dysfunction. Regional homogeneity (ReHo) is a method developed to analyze regional synchrony of spontaneous blood oxygen level-dependent fMRI signals (Wu et al. 2009; Zang et al. 2004). Thus, based on our existing work, the aim of the present study was to analyze ReHo within the resting-state ICNs, and to further understand the pathophysiological changes in adult MMD.

Methods

Participants

Twenty-six adult patients with MMD (the case group) were enrolled consecutively from January 2013 to July 2014. The criteria for inclusion included: (1) age between 18 and 80 years, right-handed; (2) diagnosis confirmed by digital subtraction angiography; (3) no abnormalities observed in the cerebral cortex, basal ganglia, brainstem, or cerebellum, but small patches of hyperintense signal neither larger than the arbitrary cutoff of 8 mm in maximum dimension on T2 images nor cystic in the cerebral subcortical white matter could be involved (Karzmark et al. 2012); (4) no evidence of recent or remote intracerebral hemorrhage; (5) no surgical intervention before recruitment; 6) physically capable of cognitive testing. Patients with significant neurological diseases or psychiatric disorders that could compromise cognition, or with other cerebrovascular diseases, severe systemic diseases, and those taking medicines such as benzodiazepine clonazepam were excluded. Angiographic staging of the case group was based on the published guidelines of Suzuki's 6-stage classification: I, narrowing of internal carotid artery (ICA) apex; II, initiation of moyamoya collaterals; III, progressive ICA stenosis with intensification of moyamoya collaterals; IV, development of external carotid artery collaterals; V, intensification of external carotid artery collaterals and reduction of moyamoya collaterals; and VI, occlusion of ICA with disappearance of moyamoya collaterals (Suzuki and Takaku 1969).

Twenty-four healthy young subjects with no memory complaints, mental diseases, any cerebrovascular disease were enrolled in the normal control (NC) group. The case and NC groups were matched on age, sex, educational background, and dominant hand.

Neuropsychological assessment

A battery of neuropsychological tests was given to the subjects by a trained neuropsychologist who was unaware of the patient diagnosis or the study aim. Among the tests, total score on Mini-Mental State Examination was for global cognition (Katzman et al. 1998), the Trail Making Test Part B (TMT-B) and a summation of executive subtests of MES (MES-EX) were for executive function (Guo et al. 2012; Lu and Bigler 2002).

Image acquisition and preprocessing

Participants were scanned using a 3.0 Tesla intraoperative MRI (iMRI) system (Siemens Medical Solutions, Erlangen, Germany). Resting-state fMRI data were obtained using gradient echo-planar imaging, time repetition/time echo =2000/35 ms; field of view =240 mm × 240 mm; matrix size =64 × 64; slice thickness = 4 mm. The scans lasted approximately 10 min. Structural images were acquired with a fast spoiled gradient recalled echo inversion recovery sequence: 1-mm thick axial section, time repetition/time echo =1000/5 ms, inversion time = 400 ms, flip angle =20°, inter-slice space =0 mm, field of view =240 mm × 240 mm, acquisition matrix =256 × 256.

Data preprocessing was performed using the SPM8 package (http://www.fil.ion.ucl.ac.uk/spm/). The first 10 volumes were discarded because of instability of the initial MRI signal. The remaining 180 volumes were carried out with slice timing correction and slice realignment for head motion correction. Functional volumes were realigned using least-squares minimization without higher-order corrections for spin history, then normalized to the Montreal Neurological Institute template. Images were warped to 3-mm isotropic voxels and then smoothed with a 4-mm full width at half maximum Gaussian kernel. Next, we performed linear trend subtraction and temporal filtering (0.01–0.08 Hz) on the time series of each voxel to reduce the effect of high-frequency noise and low-frequency drifts, by use of the Resting-State fMRI Data Analysis Toolkit (REST, http://rest.restfmri.net) (Biswal et al. 1995).

ReHo analysis

Based on the regional homogeneity hypothesis, Kendall's coefficient of concordance value (namely ReHo value) was adopted to calculate the similarity of the time series of a given voxel to its nearest 26 neighbor voxels within a functional cluster (Zang et al. 2004). Subsequently, the individual ReHo map was generated in a voxel-wise fashion and standardized into z-values (zReHo) by subtracting the mean ReHo obtained from the entire brain and dividing by the standard

deviation. Finally, the zReHo maps were spatially smoothed with a Gaussian filter and normalized to the standard Talairach atlas template.

Data processing

To generate a mask for further use, one-sample t-test was primarily performed on each subjects' zReHo maps for the case and NC groups in a voxel-wise way within the whole brain. Then, a two-sample t-test was performed to examine the between-group zReHo differences within the generated mask. Subsequently, independent component analysis was performed using the GIFT toolbox (http://icatb.sourceforge.net/) to retrieve resting-state ICNs, then the ECN, DMN, and SN were identified in accordance with a publicly available atlas of defined ICNs (http://findlab.stanford.edu/functional_ROIs.html) (Shirer et al. 2012). After extracting the voxel-based zReHo of ICNs in each participant, the data were compared between the case and NC groups using an independent samples t-test. In addition, to determine the relationship between the changes of ICNs and the disease severity, we further subdivided the case group in accordance with the stages of MMD based on Suzuki's classification, computed the averaged zReHo of ICNs in each case and compared them among different subgroups. Finally, Pearson's correlation coefficients were computed between the averaged zReHo of ICNs and neuropsychological tests in the case group. Significant threshold was set at corrected $p < 0.05$ (determined by Monte Carlo simulations with the AFNI AlphaSim program).

Statistical analysis

Database management and statistical analyses were performed via SPSS16.0 software (SPSS Inc., Chicago, IL, USA). Continuous variables were expressed as percentages or the means ± SD. Overall differences among the subgroups were assessed with one-way analysis of variance (ANOVA). Post hoc pairwise comparisons between subgroups were assessed using the LSD test. The level of significance was set at 0.05.

Results

Demographic and neuropsychological features

Initial clinical presentation leading to the enrollment in the study was transient ischemic attack in 14 patients (53.9 %); minor stroke without detectable big patches in 7 patients (26.9 %); and headache in 5 patients (19.2 %). Presenting symptoms were predominantly motor and sensory deficits (18/26); other symptoms included slow speech (4/26), syncope (3/26), and mental slowing (3/26). According to the Suzuki's 6-stage classification, 5 patients (19.2 %) were stage II, 12 patients (46.2 %) were stage III, 7 patients (26.9 %) were stage IV, and the remaining 2 patients (7.7 %) were stage V.

The case and NC groups did not significantly differ in age, sex distribution, and education level (Table 1). As expected, the case group exhibited significantly lower scores in the Mini-Mental State Examination than the NC group. With respect to the executive function, the case group performed worse than the NC group in the time consumption of the TMT-B and a summation of MES-EX scores. The two tests correlated well ($r = -0.650$; $p < 0.001$). Of note, three patients (11.5 %) in the present study could not complete the TMT-B because of illiteracy. Using of the Kruskal–Wallis test, scores of these 3 tests were compared among patients in different stages of Suzuki's classification. Results demonstrated that with the advance of the stage of MMD, patients performed worse in all 3 tests (MMSE, $\chi^2 = 19.619$, $p < 0.001$; TMT-B, $\chi^2 = 8.107$, $p = 0.044$; MES-EX, $\chi^2 = 11.545$, $p = 0.009$).

Whole brain zReHo differences between the case and NC groups

Figure 1 shows the whole brain zReHo differences between the case and NC groups (corrected $p < 0.05$). Compared with the NC group, the case group exhibited significantly decreased zReHo in the left dorsolateral prefrontal cortex (DLPFC), right medial superior frontal gyrus, right medial orbitofrontal gyrus, left inferior parietal gyrus (IPG), right superior frontal gyrus (SFG), and right supplemental motor area. Furthermore, significantly increased zReHo was noted

Table 1 Demographic and neuropsychological features of the 2 groups

Index	Case group (n = 26)	NC group (n = 24)	$t/z/X^2$ value (p value)
Age (years)	40.2 ± 9.4	40.2 ± 6.5	0.021 (0.983)
Male (%)	12 (46.2)	14 (58.3)	0.742 (0.389)
Education (years)	8.1 ± 4.8	9.3 ± 3.9	0.794 (0.433)
MMSE	24.3 ± 5.7	29.2 ± 0.9	2.937 (0.003)
TMT-B (s)	164.7 ± 62.4	121.6 ± 37.5	2.187 (0.036)
MES-EX	37.5 ± 12.8	47.2 ± 4.4	3.075 (0.002)

MMSE Mini-mental state examination; TMT-B (s) Time consumed in the trail making test part B; MES-EX The executive subtests of memory and executive screening

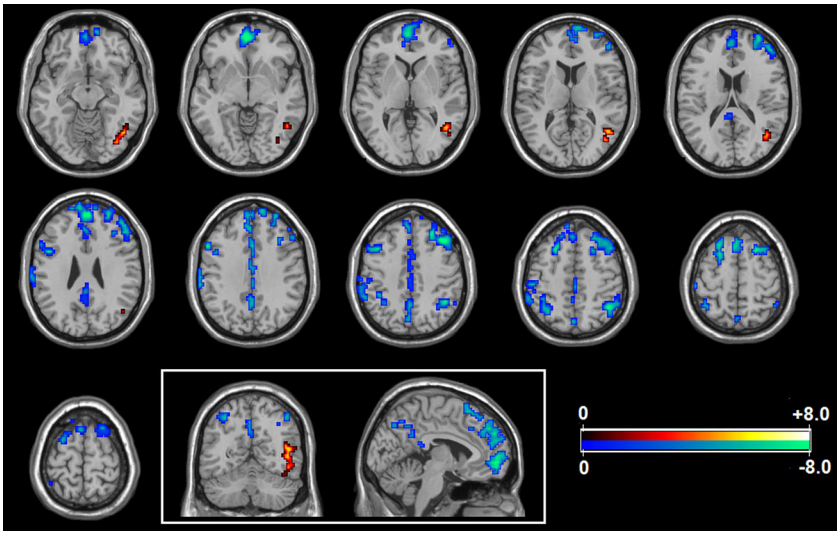

Fig. 1 Whole brain zReHo differences between the case and NC groups. Compared with the NC group, the case group exhibited significantly decreased zReHo in the left dorsolateral prefrontal cortex (DLPFC), right medial superior frontal gyrus, right medial orbitofrontal gyrus, left inferior parietal gyrus, right superior frontal gyrus, and right supplemental motor area. Additionally, significantly increased zReHo was noted in the left middle temporal gyrus. Statistical significance threshold was set at corrected $p < 0.05$ (determined by Monte Carlo simulations with the AFNI AlphaSim program)

in the left middle temporal gyrus. A detailed list of the regions is in Table 2.

ZReHo differences of ICNs at rest between the case and NC groups

Voxel-based zReHo differences of bilateral ECNs, DMN and SN at rest between the two groups are presented in Fig. 2 (corrected $p < 0.05$). Compared with NC, the case group exhibited significantly decreased zReHo in the DLPFC and IPG of left ECN, the IPG, SFG and DLPFC of the right ECN, the right precuneus, left medial superior frontal gyrus, right medial orbitofrontal gyrus of the DMN, as well as the left middle frontal gyrus and right supplemental motor area of SN. A detailed list of the regions is in Table 3.

Table 2 Whole brain ReHo differences between the case and NC groups

Brain regions	Vol (mm^3)	MNI coordinates (mm)			Maximum T
		x	y	z	
Left DLPFC	10,638	−39	24	42	−6.025
Right mSFG	3672	−3	51	24	−4.947
Right mOFG	1674	3	54	−6	−4.732
Left IPG	2349	−39	−54	45	−4.447
Right SFG	2592	24	18	51	−4.126
Right SMA	2241	39	−54	54	−3.812
Left MTG	1323	−39	−69	−18	3.088

X, y, z coordinates of primary peak locations in the MNI space; T statistical value of peak voxel showing significant differences (negative values indicate case < NC and vice versa, corrected $p < 0.05$). DLPFC Dorsolateral prefrontal cortex; mSFG Medial superior frontal gyrus; mOFG Medial orbitofrontal gyrus; IPG Inferior parietal gyrus; SMA Supplemental motor area; MTG Middle temporal gyrus

Averaged zReHo changes of ICNs according to stages of Suzuki's classification

Figure 3 shows the averaged zReHo differences of ICNs among the subgroups of patients. Results indicated that all the four ICNs exhibited a pattern of $zReHo_{II} > zReHo_{III} > zReHo_{IV} > zReHo_{V}$, but significant differences only existed in the bilateral ECNs (left, $F = 9.653$, $p < 0.001$; right, $F = 6.471$, $p = 0.003$).

Further comparison revealed that in the left ECN, there were significant differences between the stage II and other stages (III, $p = 0.010$; IV, $p < 0.001$; V, $p < 0.001$), between the stage III and other stages (IV, $p = 0.022$; V, $p = 0.012$), but not between the stage IV and stage V ($p = 0.259$). While in the right ECN, significant differences were observed between the stage II and other stages (IV, $p = 0.001$; V, $p = 0.007$), but not between stage II and stage III ($p = 0.064$), between the stage III and stage IV ($p = 0.013$), but not between stage III and stage V ($p = 0.072$), stage IV and stage V ($p = 0.847$).

Neurocognitive correlates with averaged zReHo of aberrant ICNs

Pearson's correlation coefficients were computed between the averaged zReHo of these ICNs and tests of executive functioning. Results showed that significant correlations with TMT-B (Fig. 4) and MES-EX (Fig. 5) were only observed in

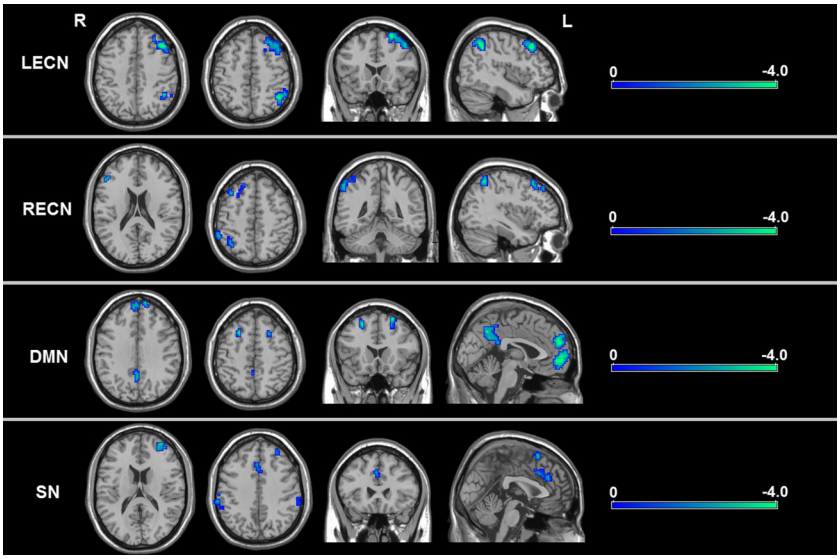

Fig. 2 Voxel-based zReHo differences of ICNs at rest between the case and NC groups. Compared with the NC group, the case group exhibited significantly decreased zReHo in the DLPFC and inferior parietal gyrus of the left ECN, the inferior parietal gyrus, superior frontal gyrus, and DLPFC of the right ECN, the right precuneus, left medial superior frontal gyrus, right medial orbitofrontal gyrus of the DMN, as well as the left middle frontal gyrus and right supplemental motor area of SN. Statistical significance threshold was set at corrected $p < 0.05$ (determined by Monte Carlo simulations with the AFNI AlphaSim program)

the left ECN ($r = -0.755$, $p < 0.001$; $r = 0.524$, $p = 0.006$, separately) and right ECN ($r = -0.442$, $p = 0.034$; $r = 0.541$, $p = 0.004$, separately).

Discussion

To date, only a limited number of published studies have focused on abnormal functional connectivity of executive function in adult MMD. By use of ReHo analysis, the present study revealed a widespread decrease of coherence of spontaneous neuronal activity in adult patients with MMD. When referring to the resting-state ICNs of bilateral ECNs, DMN, and SN, most regions that showed a statistically significant ReHo decrease belonged to these ICNs. In addition, the trend of ReHo decrease was in accordance with the disease severity in all these ICNs, but only the bilateral ECNs reached statistical significance. Finally, only bilateral ECNs exhibited significant correlations with neuropsychological tests of executive functioning.

Recent studies using both model-based and model-free approaches have revealed that the functional network of ECN, also referred to as the frontoparietal networks, involves mainly

Table 3 ReHo differences between the case and NC Groups in each ICN at rest

ICNs	Brain regions	Vol (mm^3)	MNI coordinates (mm)			Maximum T
			x	y	z	
LECN	Left DLPFC	4482	−39	24	42	−6.025
	Left IPG	1755	−39	−54	45	−4.447
RECN	Right IPG	918	39	−54	54	−3.812
	Right SFG	567	24	21	54	−3.730
	Right DLPFC	1026	39	21	48	−2.924
DMN	Right precuneus	945	3	−60	39	−5.028
	Left mSFG	1863	−3	51	24	−4.947
	Right mOFG	1566	3	54	−6	−4.732
SN	Left MFG	1512	−27	51	27	−4.873
	Right SMA	1269	66	−27	30	−3.436

X, y, z coordinates of primary peak locations in the MNI space; T statistical value of peak voxel showing significant differences (negative values indicate case < NC and vice versa, corrected $p < 0.05$). LECN Left executive control network; RECN Right executive control network; DMN Default mode network; SN Salience network; DLPFC Dorsolateral prefrontal cortex; IPG Inferior parietal gyrus; mSFG Medial superior frontal gyrus; mOFG Medial orbitofrontal gyrus; MFG Middle frontal gyrus; SMA Supplemental motor area

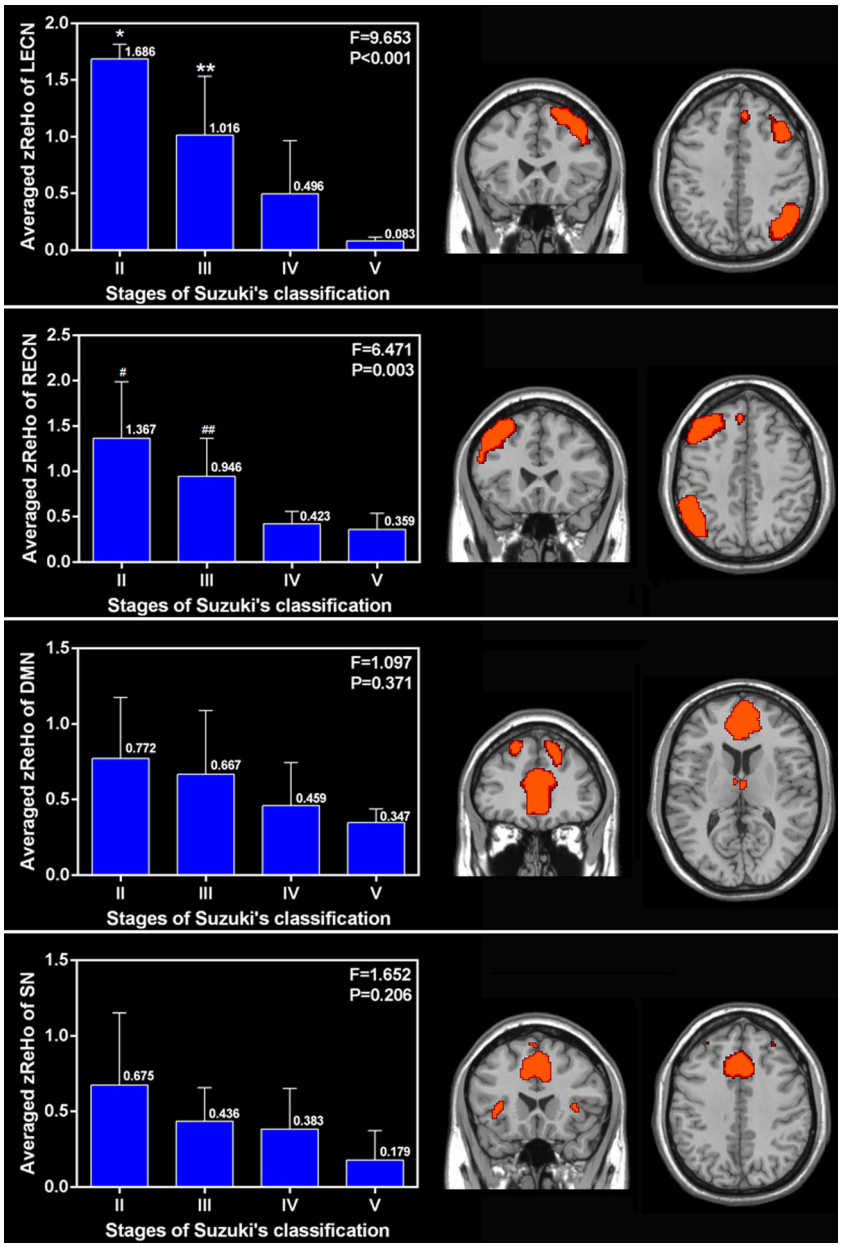

Fig. 3 Averaged zReHo differences of ICNs among different stages of Suzuki's classification. The left side of the figure indicated that all the four ICNs exhibited a pattern of $zReHo_{II} > zReHo_{III} > zReHo_{IV} > zReHo_{V}$, but significant differences only existed in the bilateral ECNs (left, $p < 0.001$; right, $p = 0.003$). The right side of the figure exhibited the publicly available atlas of defined bilateral ECNs, DMN and SN. *Significant differences between the stage II and other stages (III, $p = 0.010$; IV, $p < 0.001$; V, $p < 0.001$). **Significant differences between the stage III and other stages (IV, $p = 0.022$; V, $p = 0.012$). #Significant differences between the stage II and other stages (IV, $p = 0.001$; V, $p = 0.007$). ##Significant difference between the stage III and stage IV ($p = 0.013$)

the DLPFC, middle frontal gyrus/SFG, and posterior parietal gyrus (Cole et al. 2013; Shirer et al. 2012). Additionally, key nodes of the DMN include mainly the precuneus/posterior cingulate cortex, medial prefrontal gyrus, angular gyrus, and medial temporal gyrus (Buckner et al. 2008; Xin and Lei 2015). In addition, the SN anchors primarily in the ventrolateral prefrontal cortex, anterior insula, and anterior cingulate cortex (Seeley et al. 2007). Based on independent component analysis, our result indicates that most regions showing significant ReHo differences belong to these ICNs, implying that ECN, DMN, and SN might be the key ICNs that deteriorate in adult MMD.

Hemodynamic analysis revealed that chronic deficiencies in cerebral blood flow etiologically induced impaired executive performance in adult MMD (Calviere et al. 2010; Festa et al. 2010; Kazumata et al. 2015). Schubert et al. (2014) also indicated that the patients with MMD exhibited a territory-specific perfusion pattern, including relatively central preservation of perfusion. Among the four ICNs, the bilateral ECNs were relatively far away from the central territory of brain and only bilateral ECNs were found to exhibit significant decrease of coherent neuronal signals with disease severity. These results along with the result that patients exhibited a widespread ReHo decrease in all four ICNs, demonstrate an obvious link between hemodynamic defects and aberrant ECN, DMN, and SN and suggest that the bilateral ECNs primarily deteriorate with disease progression.

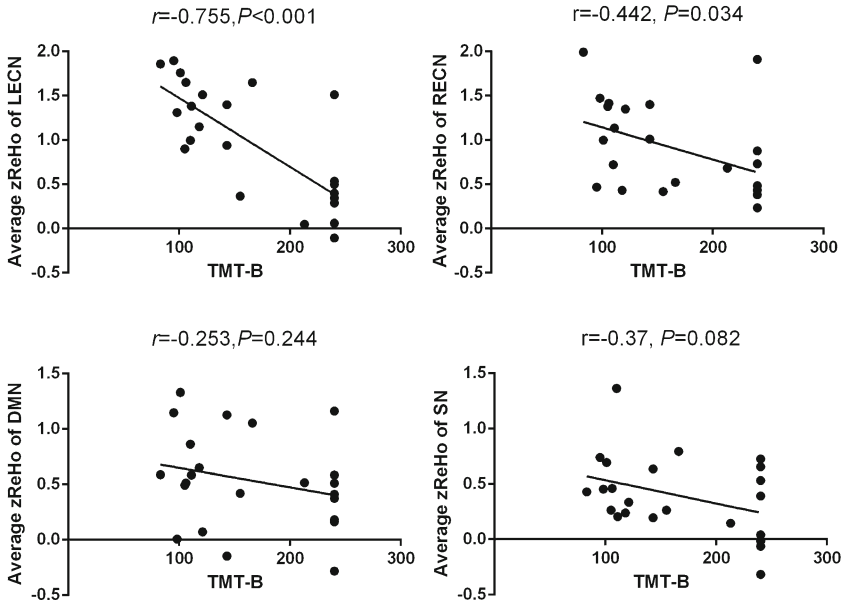

Fig. 4 Scatter plot of averaged zReHo of ICNs according to time consumption of TMT-B. Significant correlations were noted only in bilateral ECNs (left, $r = -0.755$, $p < 0.001$; right, $r = -0.442$, $p = 0.034$)

By evaluating functional interactions within and between each of these ICNs, previous studies have found that the ECN and DMN operate in a competitive relationship during task performance and that the ECN suppresses the DMN to reallocate cognitive resources from internal irrelevant thoughts and focus on goal-directed tasks (Vincent et al. 2008; Xin and Lei 2015). Furthermore, Liang et al. (2015) and Sridharan et al. (2008) reported that when cognitive load increases, functional connectivity decreases within the DMN, while it increases within the ECN, and the SN connects more with both ICNs to allocate resources to the most homeostatically salient events. However, most studies published to date are based on health participants; thus, it is still unclear how these ICNs interact functionally. The present study examines adult patients with MMD and shows that all these ICNs exhibit decreased regional coherence of spontaneous neuronal activity. Furthermore, we observed that only bilateral ECNs manifest significantly positive correlations of regional homogeneity with executive control performance. Thus, we suggest that the underlying neural mechanism may involve two factors: the direct damage of ICNs, especially bilateral ECNs, caused by chronic ischemia, and also the secondary topological reorganization of these ICNs.

Limitation

First, the study is cross-sectional with a small sample size; therefore, we were not able to subdivide patients on the basis of executive dysfunction and to further detect neurocognitive

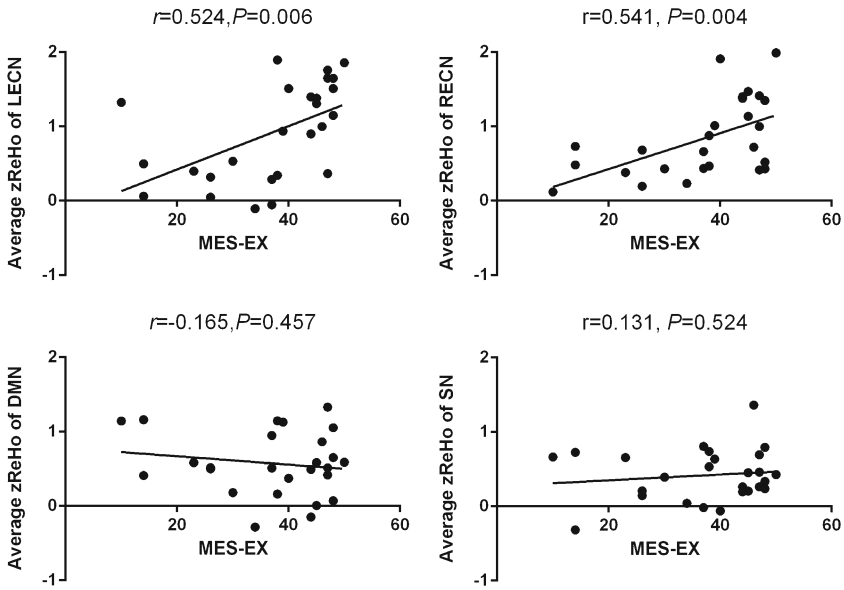

Fig. 5 Scatter plot of averaged zReHo of ICNs according to MES-EX scores. Significant correlations were noted only in bilateral ECNs (left, $r = 0.524$, $p = 0.006$; right, $r = 0.541$, $p = 0.004$)

deterioration with progression of adult MMD. We cannot rule out the possibility that as adult MMD progresses, ReHo values of nodes within these ICNs may change, even in an opposite way. In addition, only 2 patients comprised the stage-V subgroup. Consequently, the strength of statistical power was affected when we tested the differences between subgroups. Clearly, further studies with a larger sample size are needed. Second, the current network study is a resting-state voxel-wise observation based on independent component analysis and identified with a publicly available set of regions of interest (Shirer et al. 2012). Because the underlying mechanism of interaction within/between ICNs is still unclear, task-related investigations based on region-wise approaches are required in adult patients with MMD.

Conclusion

The present study demonstrates the aberrant local connectivity within resting-state ICNs with respect to adult MMD with executive dysfunction. Further investigations are needed to better understand the pathophysiological changes in adult MMD.

Acknowledgments This work is supported by grant 2014CB541604 from the National Key Basic Research Program of China (973 Program) and grant 81371307 from the National Natural Science Foundation of China.

Compliance with ethical standards All research procedures were approved by the Institutional Ethics Committee of Huashan Hospital of Fudan University, and were conducted in accordance with the 1964 Helsinki declaration and its later amendments. All participants gave written informed consent after totally understanding the purposes of our study.

Conflicts of interest Yu Lei, Jiabin Su, Hanqiang Jiang, Qihao Guo, Wei Ni, Heng Yang, Yuxiang Gu, and Ying Mao declare that they have no conflicts of interest.

References

Biswal, B., Yetkin, F. Z., Haughton, V. M., & Hyde, J. S. (1995). Functional connectivity in the motor cortex of resting human brain using echo-planar MRI. *Magnetic Resonance in Medicine*, *34*(4), 537–541.

Bressler, S. L., & Menon, V. (2010). Large-scale brain networks in cognition: emerging methods and principles. *Trends in Cognitive Sciences*, *14*(6), 277–290.

Buckner, R. L., Andrews-Hanna, J. R., & Schacter, D. L. (2008). The brain's default network: anatomy, function, and relevance to disease. *Annals of the New York Academy of Sciences*, *1124*, 1–38.

Calviere, L., Catalaa, I., Marlats, F., Viguier, A., Bonneville, F., Cognard, C., et al. (2010). Correlation between cognitive impairment and cerebral hemodynamic disturbances on perfusion magnetic resonance imaging in European adults with moyamoya disease. Clinical article. *Journal of Neurosurgery*, *133*(4), 753–759.

Cocchi, L., Halford, G. S., Zalesky, A., Harding, I. H., Ramm, B. J., Cutmore, T., et al. (2014). Complexity in relational processing predicts changes in functional brain network dynamics. *Cerebral Cortex*, *24*(9), 2283–2296.

Cole, M. W., Reynolds, J. R., Power, J. D., Repovs, G., Anticevic, A., & Braver, T. S. (2013). Multi-task connectivity reveals flexible hubs for adaptive task control. *Nature Neuroscience*, *16*(9), 1348–1355.

Festa, J. R., Schwarz, L. R., Pliskin, N., Cullum, C. M., Lacritz, L., Charbel, F. T., et al. (2010). Neurocognitive dysfunction in adult moyamoya disease. *Journal of Neurology*, *257*(5), 806–815.

Gorelick, P. B., Scuteri, A., Black, S. E., Decarli, C., Greenberg, S. M., Iadecola, C., et al. (2011). Vascular contributions to cognitive impairment and dementia: a statement for healthcare professionals from the American heart association/American stroke association. *Stroke*, *42*(9), 2672–2713.

Guo, Q. H., Zhou, B., Zhao, Q. H., Wang, B., & Hong, Z. (2012). Memory and executive screening (MES): a brief cognitive test for detecting mild cognitive impairment. *BMC Neurology*, *12*, 119.

Karzmark, P., Zeifert, P. D., Tan, S., Dorfman, L. J., Bell-Stephens, T. E., & Steinberg, G. K. (2008). Effect of moyamoya disease on neuropsychological functioning in adults. *Neurosurgery*, *62*(5), 1048–1051 discussion 1051-1052.

Karzmark, P., Zeifert, P. D., Bell-Stephens, T. E., Steinberg, G. K., & Dorfman, L. J. (2012). Neurocognitive impairment in adults with moyamoya disease without stroke. *Neurosurgery*, *70*(3), 634–638.

Katzman, R., Zhang, M. Y., Ouang-Ya-Qu, W. Z. Y., Liu, W. T., Yu, E., et al. (1998). A Chinese version of the mini-mental state examination; impact of illiteracy in a Shanghai dementia survey. *Journal of Clinical Epidemiology*, *41*(10), 971–978.

Kazumata, K., Tha, K. K., Narita, H., Kusumi, I., Shichinohe, H., Ito, M., et al. (2015). Chronic ischemia alters brain microstructural integriy and cognitive performance in adult moyamoya disease. *Stroke*, *46*(2), 354–360.

Lei, Y., Li, Y. J., Ni, W., Jiang, H. Q., Yang, Z., Guo, Q. H., et al. (2014). Spontaneous brain activity in adult patients with moyamoya disease: a resting-state fMRI study. *Brain Research*, *1546*, 27–33.

Liang, X., Zou, Q. H., He, Y., & Yang, Y. H. (2015). Topologically reorganized connectivity architecture of default-mode, executive-control, and salience networks across working memory task loads. *Cerebral Cortex*. doi:10.1093/cercor/bhu316.

Lu, L., & Bigler, E. D. (2002). Normative data on trail making test for neurologically normal, Chinese-speaking adults. *Applied Neuropsychology*, *9*(4), 219–225.

Schubert, G. A., Czabanka, M., Seiz, M., Horn, P., Vajkoczy, P., & Thomé, C. (2014). Perfusion characteristics of moyamoya disease: an anatomically and clinically oriented analysis and comparison. *Stroke*, *45*(1), 101–106.

Seeley, W. W., Menon, V., Schatzberg, A. F., Keller, J., Glover, G. H., Kenna, H., et al. (2007). Dissociable intrinsic connectivity networks for salience processing and executive control. *The Journal of Neuroscience*, *27*(9), 2349–2356.

Shirer, W. R., Ryali, S., Rykhlevskaia, E., Menon, V., & Greicius, M. D. (2012). Decoding subject-driven cognitive states with whole-brain connectivity patterns. *Cerebral Cortex*, *22*(1), 158–165.

Sridharan, D., Levitin, D. J., & Menon, V. (2008). A critical role for the right fronto-insular cortex in switching between central-executive and default-mode networks. *Proceedings of the National Academy of Sciences of the United States of America*, *105*(34), 12569–12574.

Suzuki, J., & Takaku, A. (1969). Cerebrovascular "moyamoya" disease. Disease showing abnormal net-like vessels in base of brain. *Archives of Neurology*, *20*(3), 288–299.

Vincent, J. L., Kahn, I., Snyder, A. Z., Raichle, M. E., & Bucker, R. L. (2008). Evidence for a frontoparietal control system revealed by intrinsic functional connectivity. *Journal of Neurophysiology*, *100*(6), 3328–3342.

Weinberg, D. G., Rahme, R. J., Aoun, S. G., Batjer, H. H., & Bendok, B. R. (2011). Moyamoya disease: functional and neurocognitive outcomes in the pediatric and adult populations. *Neurosurgical Focus*, *30*(6), E21.

Wu, T., Long, X. Y., Zang, Y. F., Wang, L., Hallett, M., Li, K. C., et al. (2009). Regional homogeneity changes in patients with Parkinson's disease. *Human Brain Mapping*, *30*(5), 1502–1510.

Xin, F., & Lei, X. (2015). Competition between frontoparietal control and default networks supports social working memory and empathy. *Social Cognitive and Affective Neuroscience*. doi:10.1093/scan/nsu160.

Zang, Y. F., Jiang, T. Z., Lu, Y. L., He, Y., & Tian, L. X. (2004). Regional homogeneity approach to fMRI data analysis. *NeuroImage*, *22*(1), 394–400.